NASA MEMO 1-25-59L

NASA

MEMORANDUM

EFFECT OF CONVEX LONGITUDINAL CURVATURE ON THE PLANING CHARACTERISTICS OF A SURFACE WITHOUT DEAD RISE

By Elmo J. Mottard

Langley Research Center
Langley Field, Va.

NATIONAL AERONAUTICS AND SPACE ADMINISTRATION
WASHINGTON
February 1959

NATIONAL AERONAUTICS AND SPACE ADMINISTRATION

MEMORANDUM 1-25-59L

EFFECT OF CONVEX LONGITUDINAL CURVATURE ON THE PLANING CHARACTERISTICS OF A SURFACE WITHOUT DEAD RISE

By Elmo J. Mottard

SUMMARY

A hydrodynamic investigation was made in Langley tank no. 1 of a planing surface which was curved longitudinally in the shape of a circular arc with the center of curvature above the model and had a beam of inches and a radius of curvature of 20 beams. The planing surface had length-beam ratio of 9 and an angle of dead rise of 0°. Wetted length, resistance, and trimming moment were determined for values of load coefficient C_{Δ} from -4.2 to 63.9 and values of speed coefficient C_V from 6 to 25.

The effects of convexity were to increase the wetted length-beam ratio (for a given lift), to decrease the lift-drag ratio, to move the center of pressure forward, and to increase the trim for maximum lift-drag ratio as compared with values for a flat surface. The effects were greatest at low trims and large drafts. The maximum negative lift coefficient $C_{L,b}$ obtainable with a ratio of the radius of curvature to the beam of 20 was -0.02. The effects of camber were greater in magnitude for convexity than for the same amount of concavity.

INTRODUCTION

The Langley Research Center of NASA has extended a general program of research on planing surfaces to include an investigation on the effect of longitudinal convexity. In the present paper the experimental hydrodynamic force data are presented for a circular-arc convex planing surface having zero angle of dead rise and a radius of curvature of 20 beams. Experimental results for a flat planing surface (without longitudinal curvature) are presented in reference 1.

SYMBOLS

b	beam of planing surface, ft
$C_{D,b}$	drag coefficient based on square of beam, $\frac{R}{\frac{1}{2}\rho V^2 b^2}$
$C_{D,S}$	drag coefficient based on area of chordal plane of mean wetted arc, $\frac{R}{\frac{1}{2}\rho V^2 l_{m,c} b}$ or $\frac{C_{D,b}}{l_{m,c}/b}$
$C_{f,a}$	skin-friction coefficient based on approximate mean velocity, $\frac{F_f}{\frac{1}{2}\rho V_{m,a}{}^2 S}$
$C_{f,V}$	skin-friction coefficient based on forward speed, $\frac{F_f}{\frac{1}{2}\rho V^2 S}$ or $\frac{M}{\frac{1}{2}\rho V^2 S r}$
$C_{L,b}$	lift coefficient based on square of beam, $\frac{F_v}{\frac{1}{2}\rho V^2 b^2}$ or $\frac{2C_\Delta}{C_V{}^2}$
$C_{L,S}$	lift coefficient based on area of chordal plane of mean wetted arc, $\frac{F_v}{\frac{1}{2}\rho V^2 l_{m,c} b}$ or $\frac{C_{L,b}}{l_{m,c}/b}$
C_R	resistance coefficient, R/wb^3
C_V	speed coefficient or Froude number, $V/\sqrt{gb}$
C_Δ	load coefficient or beam loading, F_v/wb^3
d	draft of trailing edge referred to undisturbed water surface, ft

d_c draft of trailing edge of chord of mean wetted arc referred to undisturbed water surface, ft

F_f friction force tangential to the planing surface, $\frac{M}{r}$, lb

F_v vertical force, lb

g acceleration due to gravity, 32.2 ft/sec^2

l_m length of arc between front and rear mean boundaries of wetted area, ft

$l_{m,1}$ length of arc between trailing edge and front mean boundary of wetted area, ft

$l_{m,2}$ length of arc between trailing edge and rear mean boundary of wetted area, ft

$l_{m,c}$ length of chord between front and rear mean boundaries of wetted area, ft

$l_{p,c}$ distance along mean chord from rear mean boundary of wetted area to intersection with resultant force vector,

$$\frac{1}{2} l_{m,c} + \sqrt{r^2 - \left(\frac{l_{m,c}}{2}\right)^2} \tan\left(\tan^{-1}\frac{R}{F_v} - \tau_c\right) + \frac{M}{F_v} \cos\left(\tan^{-1}\frac{R}{F_v}\right) \sec\left(\tan^{-1}\frac{R}{F_v} - \tau_c\right)$$

M trimming moment about center of curvature, lb-ft

p pressure on planing surface, lb/sq ft

p_{av} arithmetic mean pressure, $\frac{\int p\, dS}{S}$, lb/sq ft

r radius of curvature of planing-surface bottom, ft

R horizontal force, lb

$N_{Re,a}$ Reynolds number based on approximate mean velocity, $\frac{V_{m,a} l_m}{\nu}$

S principal wetted area (bounded by chines, heavy spray line, and trailing edge or line of separation), $l_m b$, sq ft

V speed, fps

$V_{m,a}$ approximate mean velocity over planing surface, $\sqrt{V^2\left(1 - \frac{C_{L,b}}{\frac{l_{m,c}}{b}\cos \tau_c}\right)}$, fps

w specific weight of water, lb/cu ft

ρ mass density of water, slug/cu ft

τ trim (angle between tangent at trailing edge and horizontal), deg

τ_c trim of mean chord (angle between the chord of the mean wetted arc and horizontal), deg

ν kinematic viscosity, ft^2/sec

DESCRIPTION OF MODEL

The beam of the planing-surface model was 4 inches; the length, 36 inches; and the angle of dead rise, 0°. The bottom was curved longitudinally, with the center of curvature above the model. From the view beneath the model, this curvature was convex. The radius of curvature was 80 inches. A sketch of the bottom and the cross section of the model are shown in figure 1. The model was constructed of steel with plastic covering. The planing bottom was white plastic with black lines at every inch to facilitate reading wetted lengths. The mean radius of curvature of the chines was less than 0.004 inch.

APPARATUS AND PROCEDURE

Tests

The tests were conducted in Langley tank no. 1 which, together with the apparatus for towing the model and the instrumentation for measuring the lift, drag, and trimming moment, has been described in reference 2. A schematic representation of the model and towing gear is presented in figure 2. The test procedures were similar to those described in reference 3.

The trim, load, and speed were held constant during each test run. The trim and draft were measured at the trailing edge of the model. The wetted lengths were obtained from photographs of the bottom similar to those presented in figure 3, supplemented by readings taken at the chine during the test runs. The tests with negative lift were made by forcing the model down to the water to initiate planing.

Data Analysis

For the purpose of evaluating the effects of camber, it is desirable to compare the cambered wetted surface with an uncambered wetted surface. If the uncambered wetted surface has the same trim and length as the chord of the wetted arc of the cambered surface, the camber may be regarded as the only alteration to the basic conditions. For such a comparison, a method of data analysis was employed which is briefly explained with the aid of figure 4, in which the represented quantities are scaled from the data for the test run depicted in figure 3(c). Front and rear "mean boundaries" were selected to facilitate representation of wetted areas and wetted chord lengths. The mean boundary was defined as a straight transverse line intersecting the wetted area in the region where the beam was not fully wetted so that on one side of the boundary, the unwetted portion bounded by the chines, the actual wetted boundary, and the mean boundary was equal in area to that of the wetted portion on the other side of the mean boundary. These mean boundaries defined an "equivalent" rectangle equal in area to the actual wetted area. The locations of the front and rear mean boundaries $l_{m,1}$ and $l_{m,2}$ were determined from the measurements on the photographs of the bottom such as those in figure 3 and the readings of the wetted length at the chine.

The mean chord was defined as a longitudinal straight line between the front and rear mean boundaries. The length of the mean chord $l_{m,c}$ was computed from the locations of the front and rear mean boundaries $l_{m,1}$ and $l_{m,2}$. It may be noted that the difference between the arc wetted length $\frac{l_{m,1} - l_{m,2}}{b}$ and the chord wetted length $\frac{l_{m,c}}{b}$ was very small $\left(\text{maximum, 0.33 percent when } \frac{l_{m,c}}{b} = 6\right)$.

The trim of the mean chord τ_c was computed from the trailing-edge trim τ and the locations of the mean boundaries $l_{m,1}$ and $l_{m,2}$. The draft of the trailing edge of the mean wetted arc d_c was computed from the draft of the model trailing edge d, the trailing-edge trim τ, and the location $l_{m,2}$ of the rear mean boundary.

As in reference 1, buoyant effects have not been subtracted out of the data, but large buoyant effects have been excluded by including only test runs with buoyant force less than 20 percent of the total vertical force.

Because of the circular-arc curvature of the model, only tangential forces can cause a moment about the center of curvature. It is therefore possible to obtain resultant friction force by dividing the moment about the center of curvature by the radius of curvature. In the absence of pressure data the mean velocity, and therefore also the friction coefficient and Reynolds number, were approximated. In the calculation of the approximate mean velocity, the mean pressure on the planing surface was assumed equal to

$$\frac{\text{Total lift}}{\text{Horizontal projection of wetted area}}$$

In order to assist in interpretation of the experimental results, an adaptation of airfoil theory to planing surfaces is given in the appendix.

RESULTS AND DISCUSSION

The data are presented in table I in the conventional nondimensional forms.

At trailing-edge trim settings of 5.75° or more, the flow appears to be similar to flat-plate flow, as shown by the underwater photograph in figure 3(a). At lower trim settings, the principal wetted area at the rear tapers toward the center line (fig. 3(b)). The length of the tapered area increases as the trim is decreased (a decrease in trim may be regarded as an extension rearward of the model along its arc). At the trim settings of -5.75° to -11.75°, the trailing edge of the model is behind the principal wetted area, which converges to a point, as shown in figure 3(c). The flow, in following the model, requires vertical divergence at the rear. The vertical divergence occurs near a free (constant-pressure) surface which prevents appreciable slowing down in the flow. It is therefore accompanied by a horizontal convergence, which is apparent in figure 3(c).

The data are plotted in figures 5, 6, 7, and 8. When plotted against the lift coefficient $C_{L,b}$, the nondimensional wetted length $l_{m,c}/b$ (fig. 5), center-of-pressure location $l_{p,c}/b$ (fig. 6), drag coefficient $C_{D,b}$ (fig. 7), and draft d_c/b (fig. 8) fall along a single line for each trim. Negative lift was obtained at trims of -5.75°

to -11.75° but was limited to lift coefficients of -0.02. At trailing-edge trims more negative than -5.75°, the data are the same as at -5.75° because the flow is not influenced by the trailing-edge trim. At trailing-edge trims more negative than -5.75° and values of $C_{L,b}$ near zero, the location of the center of pressure $l_{p,c}$ (fig. 6) varies greatly with $C_{L,b}$, evidently approaching positive or negative infinity as the resultant force vector approaches parallelism with the mean chord line from the direction of positive or negative lift. This type of result does not exist for a prismatic surface but may be obtained on a convex surface because of the existence of both positive and negative pressures. (See eq. (1) of appendix.)

In figure 9 the nondimensional length $\frac{l_{m,c}}{b}$ of the line between the front and rear mean boundaries is plotted against $C_{L,b}$ for various values of the trim of this line. The dashed lines are flat-plate results from reference 1. The convex surface was, of course, the poorer lifting device. The decrease in lift coefficient was least (about 11 to 14 percent) at 30° trim because of the smallness of the effect of camber relative to the effect of angle of attack at high trim. (See eq. (2) of appendix.) At lower trim the influence of the camber was greater and a greater decrease in lift occurred. For a given trim the convexity (expressed as a percentage of the chord) increased with $\frac{l_{m,c}}{b}$ as indicated by equation (3) in the appendix, causing an increase in the loss of lift when compared with a flat plate. However, at very high values of $\frac{l_{m,c}}{b}$, which are different for each trim, the effect of the convexity on the lift appears to decrease. For example, at $\tau_c = 9°$, the difference between the $C_{L,b}$ of the convex and flat surfaces increases from 8 percent at $\frac{l_{m,c}}{b} = 0.9$ to a maximum of 27 percent at $\frac{l_{m,c}}{b} = 3.6$, and decreases to 23 percent at $\frac{l_{m,c}}{b} = 5.6$. Since the lift due to camber may depend only upon the longitudinal flow component, it is not surprising that the camber loses effectiveness at large values of $\frac{l_{m,c}}{b}$, where a larger proportion of the total lift is obtained from the crossflow.

At $\tau_c = 0$ the lift was negative. The lower end of the $\tau_c = 0$ curve represents the maximum negative lift obtainable under the conditions of the test. Since the condition of maximum negative lift is unstable with a constant load, this condition could not be maintained but was approached as nearly as possible.

Since an increase in wetted length l_m at constant τ results in an increase in τ_c, the curves of τ_c = Constant may be traversed only by regarding each increase in wetted length as accompanied by a compensating decrease in τ. At small values of τ_c a point is reached where the trailing edge is not wetted (as in fig. 3(b)), and decreasing τ no longer compensates for increasing l_m. This limiting condition is represented in figures 9 and 10 by the upper ends of the curves for $\tau_c = 0^\circ$, 2°, 4°, 6°, which define the maximum wetted lengths obtainable.

The location of the center of pressure $\frac{l_{p,c}}{b}$ is plotted against $C_{L,b}$ in figure 10. The curves appear similar to those of figure 9 in that, for a given value of lift coefficient, an increase in $\frac{l_{m,c}}{b}$ was accompanied by a corresponding increase in $\frac{l_{p,c}}{b}$.

The center-of-pressure location $\frac{l_{p,c}}{b}$ is plotted against $\frac{l_{m,c}}{b}$ in figure 11 for the convex surface and the flat surface of reference 1. For the convex surface, the center-of-pressure location did not deviate greatly from a constant fraction of the wetted length for a given τ_c. (See eq. (4) in appendix.) At trims of 18° and greater the convex-surface data are little different from the flat-plate data. At smaller trims the center of pressure moves forward with decreasing trim. At trims of 6° and lower, the values of $\frac{l_{p,c}}{b}$ exceed values of $\frac{l_{m,c}}{b}$ (slope $> 45^\circ$); and this result indicates that suction occurs on the rear of the surface. (See eq. (1) in appendix.)

In figure 12 is plotted the nondimensional draft $\frac{d_c}{b}$ referred to the undisturbed water surface against the nondimensional draft $\frac{l_{m,c}}{b} \sin \tau_c$ referred to the water surface at the leading edge. At high trim the draft referred to the water surface at the leading edge was greater (the points lie below the dashed 45° line), so that pile-up is indicated. The results presented here are similar to those for the flat surface in reference 1, except that the flat surface gave slightly larger depression of the water surface at low trim.

The lift-drag ratios for the convex and flat surfaces are compared in figure 13. The difference in lift-drag ratios was small at small wetted length because the convexity (expressed as a percentage of the chord) was small. At greater wetted length the adverse effect of convexity was great at the trim for maximum lift-drag ratio, but rapidly

diminished with increasing trim. (See eq. (6) in appendix.) Maximum lift-drag ratio was obtained for the convex surface at about 7° of trim, compared with 5° of trim for the flat surface. This result is in agreement with equation (7) in the appendix.

In figure 14 a comparison is made of lift-drag ratios and center-of-pressure location of the convex surfaces with results obtained by Sottorf (ref. 4) for cambered planing surfaces. The flat-plate results of references 1 and 4 also are included in this figure. The effect of convexity was greater than the effect of the same amount of concavity $\left(\frac{r}{b} = 20\right)$. The effects of increasing camber (increasing camber being considered as proceeding continuously from a large degree of convexity through zero longitudinal curvature to a large degree of concavity) were to increase the lift-drag ratio, move the center of pressure rearward, and decrease the trim for maximum lift-drag ratio. The changes in lift-drag ratio and center of pressure were greatest at low trim.

It should be noted that the total friction plotted against lift in figure 15 is the difference between the rearward directed shear force acting over most of the principal wetted area and the shear force of the forward directed spray which clings to the model. The area S in the nondimensional friction expression is the principal wetted area (fig. 3) and does not include the wetted area forward of the heavy spray line. At high trim and small lift coefficient, the area wetted by spray was probably much larger than the principal wetted area, which accounts for the large negative values of the nondimensional mean friction in figure 15. Some of the scatter in the data was perhaps caused by variation of the friction with Reynolds number.

The skin-friction coefficient and Reynolds number as defined in the section on data analysis are plotted in figure 16. At low trim ($\tau_c < 6^{\circ}$) the skin-friction coefficient fell slightly below the Schoenherr value (ref. 5). At higher trims, the effect of Reynolds number on skin-friction coefficient was slight as compared with the effect of flow configuration, which was considered in the discussion of figure 15.

CONCLUDING REMARKS

The effects of convexity were to increase the wetted length-beam ratio (for a given lift), decrease the lift-drag ratio, move the center of pressure forward and increase the trim for maximum lift-drag ratio as compared with these parameters for a flat plate. The effects of convexity on length-beam ratio, lift-drag ratio, and center-of-pressure location were greatest at low trim and large draft. The maximum negative lift coefficient obtainable with a radius of curvature to beam

ratio of 20 was -0.02. The effects of camber were greater in magnitude for convexity than for the same amount of concavity.

Langley Research Center,
National Aeronautics and Space Administration,
Langley Field, Va., October 20, 1958.

APPENDIX

AIRFOIL THEORY APPLIED TO PLANING

The application of airfoil theory to planing is discussed in reference 6. The following equations for thin circular-arc airfoils at small angles of attack were adapted from reference 7. In these equations the first term on the right-hand side is due to angle of attack and the second is due to camber. The positive sign is used for a concave surface and the negative sign for a convex surface.

The chordwise lift distribution for an airfoil of infinite aspect ratio is given by

$$\frac{dC_L}{dx} = \frac{4\alpha}{c}\sqrt{\frac{c - x}{x}} \pm \frac{32f}{c^3}\sqrt{x(c - x)} \qquad (1)$$

where C_L is the lift coefficient, x is the distance from the leading edge, α is the angle of attack, c is the chord of the airfoil (comparable to the wetted length of the planing surface), and f is the height of the segment bounded by the arc and its chord. The planing lift distribution would be one-half of this amount because only the bottom side contributes lift. The first term gives a pressure distribution with positive pressures increasing toward the front and the second term gives, for a convex surface, negative pressures symmetrically distributed about the midchord. The sum of these distributions would have a positive pressure peak at the front and a lower pressure or suction at the rear.

Zero lift occurs when the total upward force of the first term is equal to the total downward force of the second. Since the resultant of the distribution given by the first term is at a distance $c/4$ from the leading edge and that of the second term $c/2$ from the leading edge, a bow-up moment exists at zero lift.

The lift for an airfoil of infinite aspect ratio is given by

$$C_L = 2\pi\alpha \pm 4\pi\frac{f}{c} \qquad (2)$$

The planing lift would be one-half of this amount.

Inasmuch as the second term of equation (2) does not change with angle of attack, an amount of camber which has a large effect at small angles of attack may be relatively ineffective at large angles of attack.

For a convex planing surface, the camber f/c is not constant but increases with the wetted length. The radius of curvature r is constant and a variation in c resulting from varying the wetted length causes f/c to vary according to the following equation:

$$\frac{f}{c} = \frac{r}{c} - \sqrt{\left(\frac{r}{c}\right)^2 - \frac{1}{4}} \tag{3}$$

The moment about the leading edge for infinite aspect ratio is given by

$$C_m = \frac{\pi}{2}\alpha \pm 2\pi \frac{f}{c} \tag{4}$$

In this equation, a moment tending to decrease the angle of attack is considered positive. For a flat plate the second term is zero and C_m depends only on the angle of attack, so the center-of-pressure location is a constant fraction of the chord for a given angle of attack. For a convex surface, the second term gives a moment which tends to increase angle of attack.

The drag produced by the sharp leading edge (analogous to the spray drag for a planing surface) is, for infinite aspect ratio, equal to $2\pi\alpha^2$. The total drag is obtained by adding the friction drag C_f. Then,

$$C_D = 2\pi\alpha^2 + C_f \tag{5}$$

and the lift-drag ratio is

$$\frac{C_L}{C_D} = \frac{2\pi\alpha \pm 4\pi \frac{f}{c}}{2\pi\alpha^2 + C_f} = \frac{\alpha \pm \frac{2f}{c}}{\alpha^2 - \frac{C_f}{2\pi}} \tag{6}$$

The effect of camber is evidently great when f/c is great and the angle of attack is small. The angle of attack for maximum lift-drag ratio α_m, obtained by setting $\frac{d(C_L/C_D)}{d\alpha} = 0$ is

$$\alpha_m = \sqrt{\left(\frac{2f}{c}\right)^2 + \frac{C_f}{2\pi}} - \left(\pm\frac{2f}{c}\right) \tag{7}$$

which shows that convexity increases the angle of attack for maximum lift-drag ratio.

REFERENCES

1. Weinstein, Irving, and Kapryan, Walter J.: The High-Speed Planing Characteristics of a Rectangular Flat Plate Over a Wide Range of Trim and Wetted Length. NACA TN 2981, 1953.

2. Truscott, Starr: The Enlarged N.A.C.A. Tank, and Some of Its Work. NACA TM 918, 1939.

3. Kapryan, Walter J., and Weinstein, Irving: The Planing Characteristics of a Surface Having a Basic Angle of Dead Rise of 20° and Horizontal Chine Flare. NACA TN 2804, 1952.

4. Sottorf, W.: Experiments With Planing Surfaces. NACA TM 739, 1934.

5. Davidson, Kenneth S. M.: Resistance and Powering. Detailed Considerations - Skin Friction. Vol. II of Principles of Naval Architecture, ch. II, pt. 2, sec. 7, Henry E. Rossell and Lawrence B. Chapman, eds., Soc. Naval Arch. and Marine Eng., 1939, pp. 76-83.

6. Wagner, Herbert: Planing of Watercraft. NACA TM 1139, 1948.

7. Betz, A.: Applied Airfoil Theory. Properties of Typical Profiles. Vol. IV of Aerodynamic Theory, div. J., ch. II, secs. 1 and 2, W. F. Durand, ed., Julius Springer (Berlin), 1935, pp. 26-31.

TABLE I.- EXPERIMENTAL DATA FOR A LONGITUDINALLY CONVEX PLANING SURFACE HAVING A RADIUS OF CURVATURE 20 TIMES THE BEAM AND 0° ANGLE OF DEAD RISE

[Average kinematic viscosity = 12.04 × 10^{-6} ft^2/sec; specific weight of tank water = 63.4 lb/cu ft]

C_Δ	C_V	C_R	$\frac{l_{m,1}}{b}$	$\frac{l_{m,2}}{b}$	$\frac{l_{m,c}}{b}$	$\frac{d_c}{b}$	$C_{L,b}$	$C_{D,b}$	$C_{L,S}$	$C_{D,S}$	$C_{f,V}$	$\frac{l_{p,c}}{b}$
τ = -11.75												
-4.26	24.55	2.74	5.52	----	----	-----	-0.0142	0.0090	-------	------	-------	-----
2.13	21.56	3.12	5.90	----	----	-----	.0092	.013+	-------	------	-------	-----
6.39	21.53	3.78	6.28	3.10	3.18	0.09	.0276	.016+	0.0087	0.0052	0.0030	5.85
19.17	21.56	6.53	7.18	3.35	3.83	.28	.0824	.028)	.0215	.0073	.0029	4.83
19.17	24.58	7.09	6.90	3.34	3.56	.23	.0634	.023+	.0178	.0066	.0030	4.72
τ = -8.75												
-2.13	15.56	1.23	4.28	1.71	2.58	-0.01	-0.0176	0.010?	-0.0046	0.0040	0.0030	-1.13
2.13	21.53	2.95	4.85	1.93	2.93	.06	.0092	.012?	.0031	.0044	.0031	10.46
8.52	18.48	3.63	5.78	2.36	3.42	.19	.0498	.021?	.0146	.0062	.0029	5.15
8.52	18.48	3.58	5.78	----	----	-----	.0498	.021)	-------	------	-------	-----
12.78	15.43	4.30	6.65	2.45	4.20	.32	.1074	.036?	.0256	.0086	.0026	5.16
14.91	24.71	5.90	5.72	2.30	3.42	.18	.0488	.019+	.0143	.0057	.0026	5.04
27.69	24.80	8.92	6.28	2.37	3.91	.30	.0900	.029)	.0230	.0074	.0026	4.74
τ = -5.75												
-2.00	12.20	0.78	----	----	----	-----	-0.0268	0.010+	-------	------	-------	-----
-2.13	15.46	1.14	3.15	0.69	2.45	0.05	-.0178	.009?	-0.0048	0.0039	0.0031	-0.81
2.13	21.59	2.99	3.78	----	----	-----	.0092	.012?	-------	------	-------	-----
6.39	6.83	2.43	7.65	----	----	-----	.2740	.104?	-------	------	-------	-----
6.39	7.78	2.42	7.15	----	----	-----	.2112	.080)	-------	------	-------	-----
6.39	8.63	2.37	6.65	----	----	-----	.1716	.063?	-------	------	-------	-----
6.39	9.58	2.36	6.28	----	----	-----	.1392	.051+	-------	------	-------	-----
6.39	10.49	2.35	5.90	----	----	-----	.1162	.042?	-------	------	-------	-----
6.39	18.57	3.04	4.40	1.00	3.40	.20	.0370	.017?	.0109	.0052	.0027	8.65
6.39	15.61	2.66	4.78	1.16	3.62	.22	.0524	.021?	.0135	.0060	.0028	5.24
10.65	8.97	3.88	7.60	----	----	-----	.2648	.096+	-------	------	-------	-----
10.65	9.27	3.88	7.40	----	----	-----	.2478	.090?	-------	------	-------	-----
10.65	10.77	3.73	6.72	----	----	-----	.1836	.064+	-------	------	-------	-----
10.65	12.29	3.67	6.15	----	----	-----	.1410	.048?	-------	------	-------	-----
10.65	15.34	3.72	5.35	----	----	-----	.0904	.031?	-------	------	-------	-----
10.65	12.26	3.63	6.15	1.63	4.51	.42	.1416	.048+	.0314	.0107	.0031	5.39
12.78	12.50	4.52	6.45	1.71	4.73	.50	.1636	.057?	.0346	.0122	.0031	4.80
14.91	15.43	5.01	5.90	1.54	4.35	.43	.1252	.042?	.0288	.0097	.0027	5.18
14.91	21.56	5.26	4.90	----	----	-----	.0642	.022?	-------	------	-------	-----
17.04	12.44	5.80	7.02	1.84	5.15	.68	.2202	.075?	.0427	.0146	.0030	5.35
19.17	12.38	6.69	7.35	1.96	5.37	.74	.2502	.087?	.0466	.0162	.0028	5.63
23.43	21.41	7.47	5.48	1.47	4.00	.36	.1022	.032?	.0255	.0082	.0027	4.74

TABLE I.- EXPERIMENTAL DATA FOR A LONGITUDINALLY CONVEX PLANING SURFACE HAVING A RADIUS OF CURVATURE 20 TIMES THE BEAM AND 0° ANGLE OF DEAD RISE - Continued

[Average kinematic viscosity = 12.04×10^{-6} ft^2/sec; specific weight of tank water = 63.4 lb/cu ft]

C_Δ	C_V	C_R	$\frac{l_{m,1}}{b}$	$\frac{l_{m,2}}{b}$	$\frac{l_{m,c}}{b}$	$\frac{d_c}{b}$	$C_{L,b}$	$C_{D,b}$	$C_{L,S}$	$C_{D,S}$	$C_{f,V}$	$\frac{l_{p,c}}{b}$
τ = -0.25												
2.13	12.32	0.77	2.09	----	----	-----	0.0280	0.0102	-------	------	-------	-----
4.26	12.38	1.44	2.90	----	----	-----	.0556	.0188	-------	------	-------	-----
4.26	24.61	1.94	1.72	----	----	-----	.0140	.0064	-------	------	-------	-----
5.11	6.22	1.85	5.65	----	----	-----	.2640	.0956	-------	------	-------	-----
6.39	12.35	1.92	3.34	----	----	-----	.0838	.0252	-------	------	-------	-----
6.39	12.20	2.02	3.48	----	----	-----	.0858	.0272	-------	------	-------	-----
10.65	12.32	3.25	4.15	----	----	-----	.1404	.0428	-------	------	-------	-----
10.65	24.80	3.54	2.34	0.05	2.30	0.06	.0346	.0116	0.0151	0.0050	0.0025	3.57
10.65	18.54	3.30	2.90	.14	2.76	.10	.0620	.0192	.0224	.0070	.0028	3.60
10.65	12.26	3.31	4.22	.18	4.02	.43	.1418	.0440	.0352	.0109	.0025	4.53
14.91	12.44	4.83	4.78	.29	4.48	.57	.1926	.0624	.0430	.0139	.0027	4.69
19.17	12.44	6.38	5.38	.44	4.94	.61	.2478	.0824	.0503	.0167	.0026	5.12
27.69	24.70	8.06	3.35	.10	3.24	.21	.0908	.0264	.0279	.0081	.0026	3.89
27.69	12.41	9.99	6.40	.48	5.90	.88	.3596	.1298	.0610	.0220	.0023	5.79
27.69	12.38	9.90	6.28	----	----	-----	.3612	.1292	-------	------	-------	-----
36.21	24.58	10.42	3.78	.24	3.54	.27	.1198	.0344	.0339	.0097	.0026	3.98
36.21	21.66	10.61	4.28	.32	3.96	.36	.1544	.0452	.0391	.0114	.0025	4.22
36.21	18.42	11.07	4.90	.44	4.46	.48	.2134	.0652	.0479	.0146	.0025	4.59
τ = 5.75												
2.13	6.22	0.43	1.35	----	1.35	0.16	0.1100	0.0222	0.0822	0.0164	0.0008	1.76
3.20	6.86	.73	1.72	----	1.72	.23	.1360	.0310	.0789	.0179	.0035	1.63
3.20	7.78	.60	1.28	----	1.28	.14	.1058	.0198	.0830	.0155	.0021	1.17
4.26	6.25	1.14	2.78	----	2.78	.44	.2182	.0584	.0786	.0210	.0024	2.62
4.26	7.81	.91	1.78	----	1.78	.23	.1396	.0298	.0786	.0167	.0014	1.84
4.26	9.33	.67	1.10	----	1.10	.08	.0978	.0154	.0889	.0140	.0008	1.16
6.39	12.41	.95	.72	----	.72	.12	.0830	.0124	.1144	.0170	.0032	.41
6.39	6.80	1.84	3.48	----	3.48	.55	.2764	.0796	.0795	.0229	.0021	3.14
6.39	7.75	1.66	2.72	----	2.72	.39	.2128	.0552	.0781	.0202	.0018	2.63
10.65	7.72	3.35	4.15	----	4.14	.73	.3574	.1124	.0864	.0271	.0016	3.75
10.65	9.28	2.85	3.10	----	3.10	.46	.2470	.0662	.0796	.0214	.0018	2.79
10.65	15.59	1.59	.72	----	.72	.04	.0876	.0130	.1210	.0178	.0024	.56
12.78	9.27	3.69	3.60	----	3.60	.57	.2974	.0858	.0826	.0238	.0018	3.14
14.91	12.50	3.39	2.28	----	2.28	.37	.1908	.0434	.0838	.0190	.0019	1.92
14.91	9.36	4.58	4.02	----	4.01	.70	.3404	.1046	.0847	.0260	.0015	3.60
14.91	15.56	2.57	1.22	----	1.22	.11	.1232	.0212	.1006	.0172	.0018	1.07
17.04	9.36	5.56	4.35	----	4.34	.75	.3890	.1270	.0896	.0293	.0022	3.80
19.17	21.78	2.67	.65	----	.65	.09	.0808	.0112	.1242	.0172	.0014	.55
19.17	15.62	3.89	1.85	----	1.85	.24	.1572	.0318	.0850	.0172	.0019	1.56
19.17	9.18	6.62	4.85	----	4.84	.94	.4548	.1572	.0940	.0325	.0020	4.25
21.30	18.85	3.70	1.22	----	1.22	.19	.1198	.0208	.0977	.0169	.0018	1.06
21.30	9.34	7.29	5.10	----	5.09	1.02	.4886	.1672	.0955	.0328	.0018	4.26
21.30	15.56	4.60	1.98	----	1.98	.23	.1760	.0380	.0891	.0192	.0021	1.77
23.43	12.41	6.76	3.58	----	3.58	.64	.3042	.0878	.0851	.0245	.0021	3.13
23.45	9.30	8.75	5.60	----	5.58	1.18	.5422	.2024	.0972	.0363	.0017	4.79
27.69	15.56	6.86	2.72	----	2.72	.40	.2288	.0566	.0840	.0207	.0020	2.40
38.34	12.50	13.64	5.15	----	5.14	1.08	.4908	.1746	.0956	.0340	.0023	4.04
42.60	18.73	10.89	2.90	----	2.90	.48	.2428	.0620	.0838	.0214	.0018	2.55
42.60	15.59	13.03	4.02	----	4.02	-----	.3506	.1072	.0872	.0267	.0020	3.50
51.12	15.62	16.93	4.65	----	4.64	.87	.4190	.1388	.0903	.0299	.0018	4.01

TABLE I.- EXPERIMENTAL DATA FOR A LONGITUDINALLY CONVEX PLANING SURFACE HAVING A RADIUS OF CURVATURE 20 TIMES THE BEAM AND 0° ANGLE OF DEAD RISE - Concluded

[Average kinematic viscosity = 12.04 × 10^{-6} ft^2/sec; specific weight of tank water = 63.4 lb/cu ft]

C_Δ	C_V	C_R	$\frac{l_{m,1}}{b}$	$\frac{l_{m,2}}{b}$	$\frac{l_{m,c}}{b}$	$\frac{d_c}{b}$	$C_{L,b}$	$C_{D,b}$	$C_{L,S}$	$C_{D,S}$	$C_{f,V}$	$\frac{l_{p,c}}{b}$
τ = 11.75												
2.13	6.28	0.56	0.48	----	0.48	0.01	0.1080	0.0284	0.2272	0.0592	0.0018	0.64
3.20	6.31	.74	.75	----	.75	.09	.1604	.0372	.2140	.0496	-.0060	.50
3.20	6.86	.73	.60	----	.60	.06	.1358	.0310	.2262	.0517	-.0064	.47
4.26	7.78	1.01	.58	----	.58	.02	.1408	.0334	.2448	.0576	-.0009	.60
6.39	6.22	1.89	1.90	----	1.90	----	.3304	.0976	.1740	.0514	.0007	1.56
6.39	6.89	1.80	1.52	----	1.52	.26	.2692	.0758	.1765	.0495	.0001	1.21
6.39	7.75	1.66	1.05	----	1.05	.16	.2128	.0552	.2028	.0526	-.0008	1.08
6.39	9.21	1.51	.60	----	.60	.06	.1506	.0356	.2510	.0593	-.0002	.58
10.65	6.25	3.71	3.38	----	3.38	----	.5452	.1900	.1614	.0562	0	2.61
11.29	7.81	3.48	2.22	----	2.23	.48	.3702	.1140	.1663	.0511	.0021	1.64
11.29	9.27	3.02	1.35	----	1.35	.24	.2650	.0702	.1963	.0520	.0017	.96
11.29	10.89	2.70	.85	----	.85	.12	.1904	.0456	.2240	.0536	-.0010	.59
11.29	12.44	2.55	.60	----	.60	.06	.1460	.0330	.2432	.0550	-.0046	.36
17.04	15.62	3.66	.52	----	.52	.12	.1396	.0300	.2660	.0566	-.0035	.40
23.43	12.41	6.46	1.68	----	1.68	.28	.3042	.0838	.1817	.0499	-.0001	1.31
25.56	15.71	6.15	.90	----	.90	.22	.2072	.0498	.2300	.0553	-.0009	.72
31.95	12.47	10.03	2.45	----	2.45	.51	.4110	.1290	.1679	.0527	.0009	1.89
42.60	18.82	10.52	1.15	----	1.15	.20	.2406	.0594	.2092	.0517	-.0016	.86
42.60	15.68	12.27	2.02	----	2.03	.40	.3466	.0998	.1711	.0492	-.0001	1.86
51.12	24.77	11.44	.65	----	.65	.12	.1666	.0372	.2562	.0572	-.0030	.54
59.64	15.74	20.04	2.98	----	2.98	.78	.4814	.1618	.1620	.0543	.0011	2.25
61.77	21.72	15.45	1.35	----	1.35	.29	.2618	.0654	.1939	.0484	-.0020	1.00
63.90	15.68	22.26	3.22	----	3.22	.77	.5198	.1810	.1611	.0560	.0013	2.45
τ = 17.75												
19.17	9.36	7.25	1.60	----	1.60	0.41	0.4376	0.1656	0.2735	0.1035	-0.0014	1.14
19.17	10.80	6.75	1.08	----	1.08	.24	.3288	.1158	.3060	.1072	-.0037	.82
19.17	12.38	6.33	.72	----	.72	.13	.2502	.0826	.3454	.1132	-.0063	.54
21.30	9.27	8.38	1.88	----	1.88	.52	.4958	.1950	.2646	.1037	-.0004	1.33
23.43	12.38	8.01	.95	----	.95	----	.3058	.1046	.3220	.1101	-.0050	.69
27.69	12.38	9.79	1.22	----	1.23	----	.3614	.1278	.2950	.1039	-.0040	.86
31.95	15.62	10.64	.75	----	.75	.15	.2620	.0872	.3494	.1163	-.0056	.55
31.95	12.32	11.75	1.45	----	1.45	----	.4210	.1548	.2902	.1068	-.0029	1.02
36.21	12.57	13.70	1.70	----	1.70	----	.4584	.1734	.2694	.1020	-.0025	1.23
40.47	15.62	14.10	1.08	----	1.08	.26	.3318	.1156	.3084	.1070	-.0039	.76
40.47	18.76	13.07	.62	----	.62	.13	.2300	.0742	.3680	.1178	-.0070	.42
40.47	12.47	15.92	2.00	----	2.00	----	.5204	.2048	.2602	.1024	-.0017	1.40
53.25	18.70	18.09	.92	----	.92	.24	.3046	.1034	.3292	.1112	-.0051	.66
53.25	25.04	16.37	.42	----	.42	----	.1698	.0522	.3994	.1214	-.0106	.19
τ = 23.75												
10.65	7.78	4.83	0.85	----	0.85	0.19	0.3518	0.1596	0.3700	0.1680	-0.0072	0.50
12.78	7.81	5.98	1.02	----	1.02	.27	.4190	.1960	.4085	.1903	-.0053	.69
14.91	7.87	7.14	1.28	----	1.28	.37	.4814	.2306	.3774	.1802	-.0044	.84
17.04	7.81	8.43	1.55	----	1.55	.48	.5586	.2764	.3600	.1783	-.0035	1.09
31.95	12.44	14.76	1.02	----	1.02	.26	.4130	.1908	.4030	.1852	-.0075	.71
40.47	12.44	19.56	1.28	----	1.28	.44	.5230	.2528	.4100	.1991	-.0051	.92
40.47	16.96	17.93	.55	----	.55	----	.2814	.1246	.5114	.2265	-.0100	.41
53.25	15.52	25.02	1.08	----	1.08	.34	.4422	.2078	.4100	.1924	-.0051	.73
τ = 29.75												
10.65	7.78	6.16	0.75	----	0.75	----	0.3518	0.2036	0.4688	0.2715	-0.0099	0.47
12.78	7.78	7.54	.92	----	.92	----	.4222	.2490	.4566	.2677	-.0084	.57
14.91	7.78	9.01	1.10	----	1.10	----	.4926	.2978	.4435	.2707	-.0065	.70
17.04	10.80	9.72	.55	----	.55	----	.2922	.1666	.5315	.3029	-.0134	.46
21.30	10.83	12.35	.75	----	.75	----	.3632	.2106	.4840	.2808	-.0103	.51
25.56	10.86	15.05	.95	----	.95	----	.4334	.2552	.4565	.2686	-.0086	.58
29.56	15.89	14.02	.35	----	.35	----	.2024	.1110	.5786	.3171	-.0191	.24

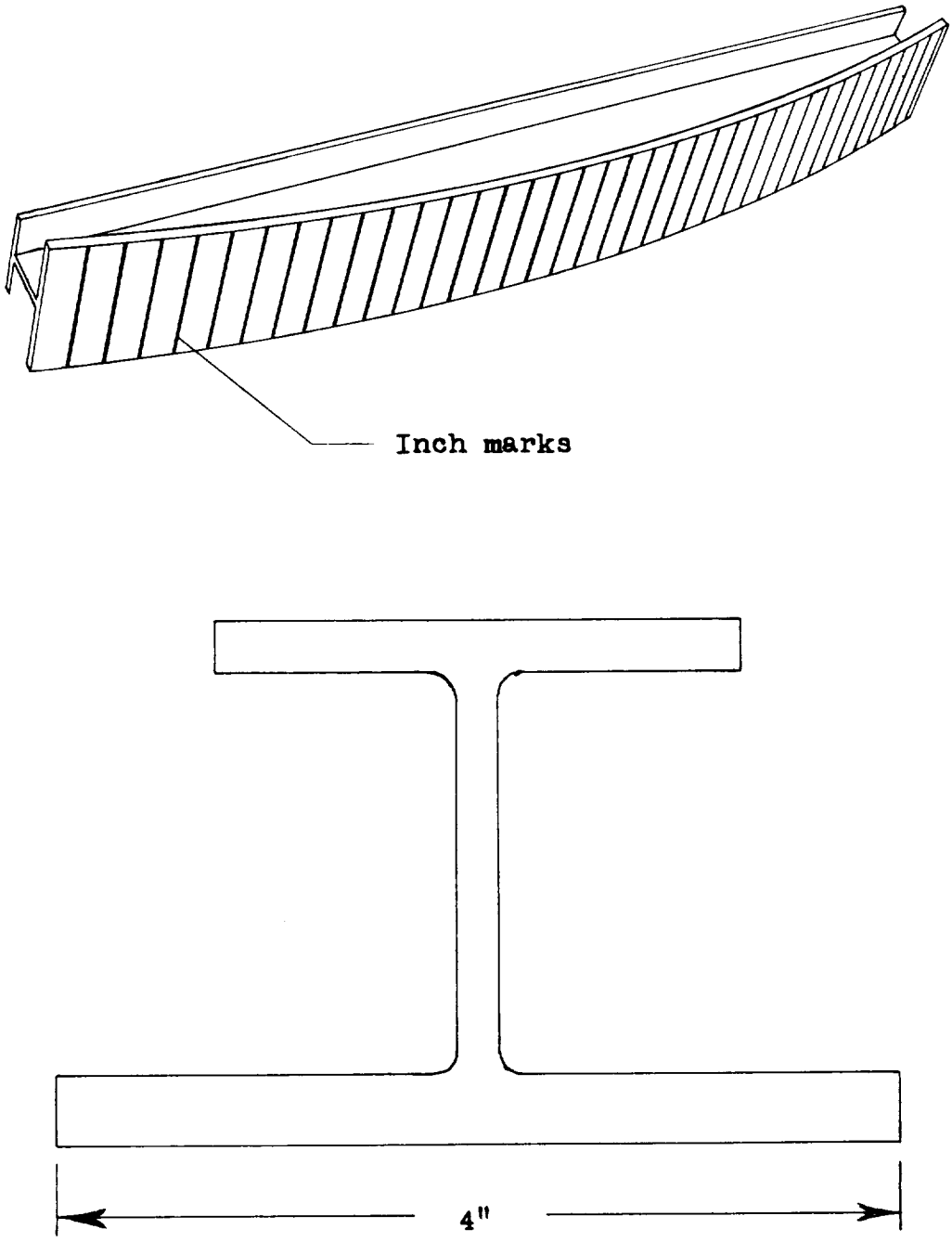

Figure 1.- Sketch and cross section of model.

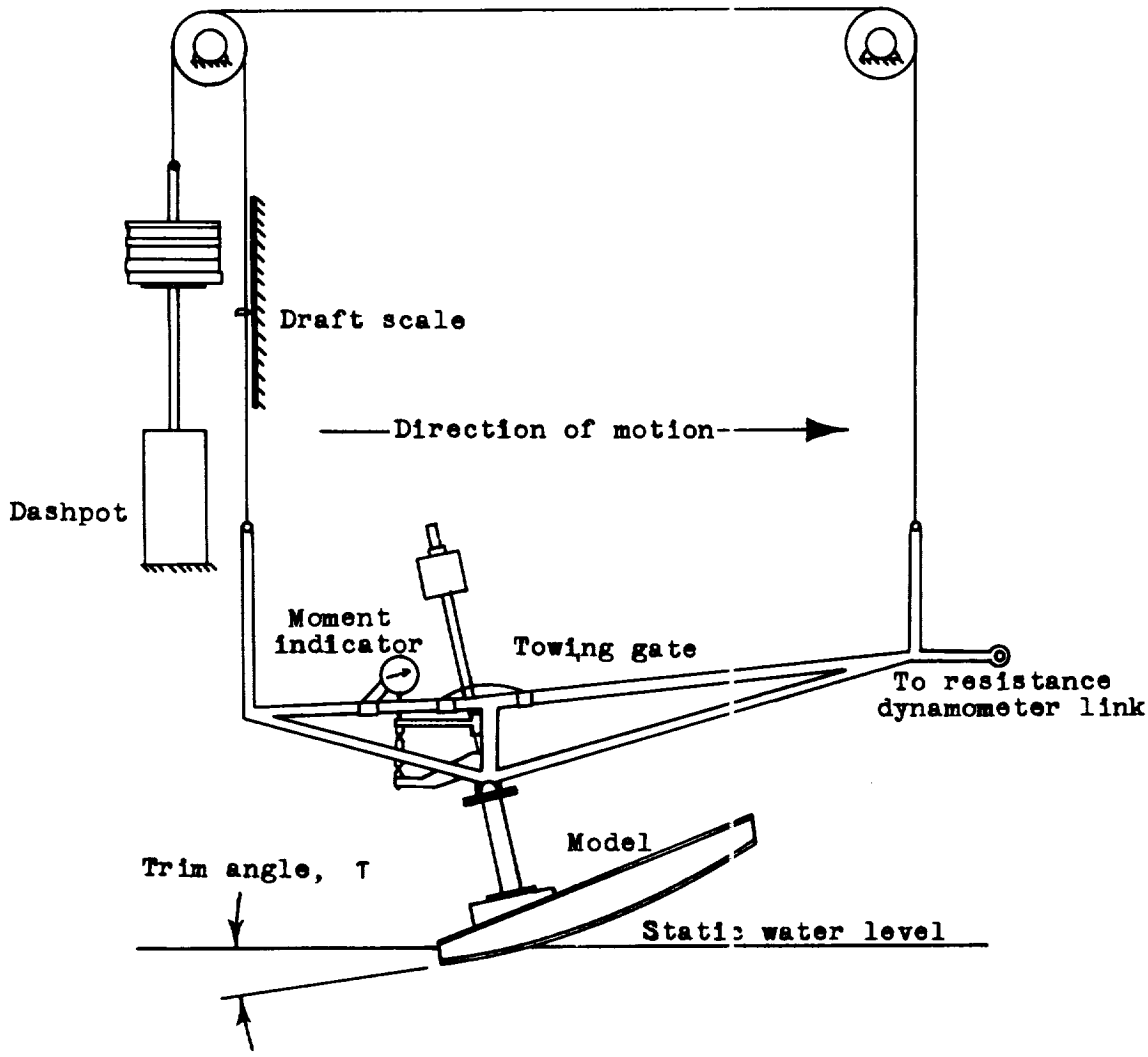

Figure 2.- Model on towing gear.

(a) At a trim τ of 5.75°. L-58-129a

Figure 3.- Typical underwater photographs.

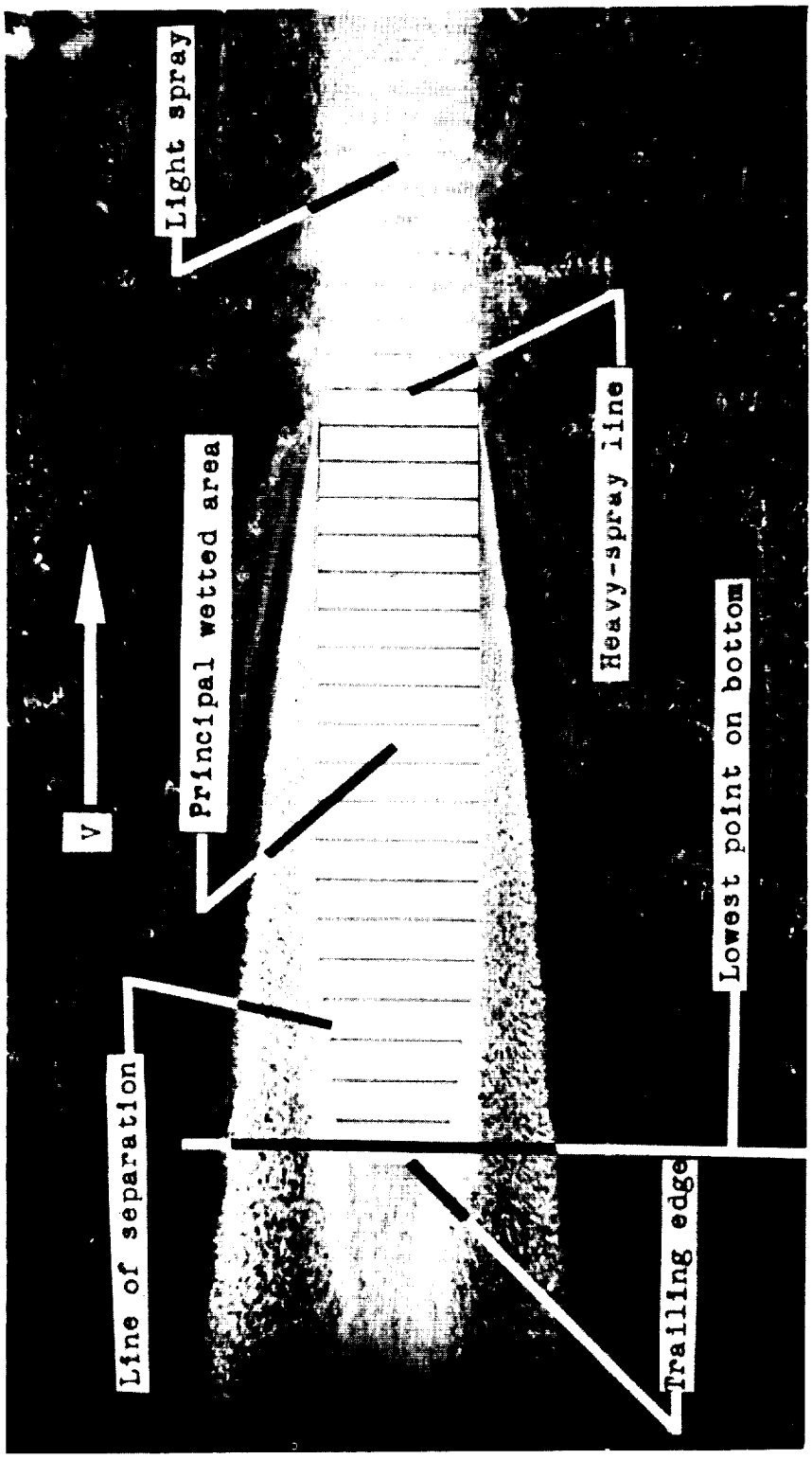

(b) At a trim τ of -0.25°. L-58-130a

Figure 3.- Continued.

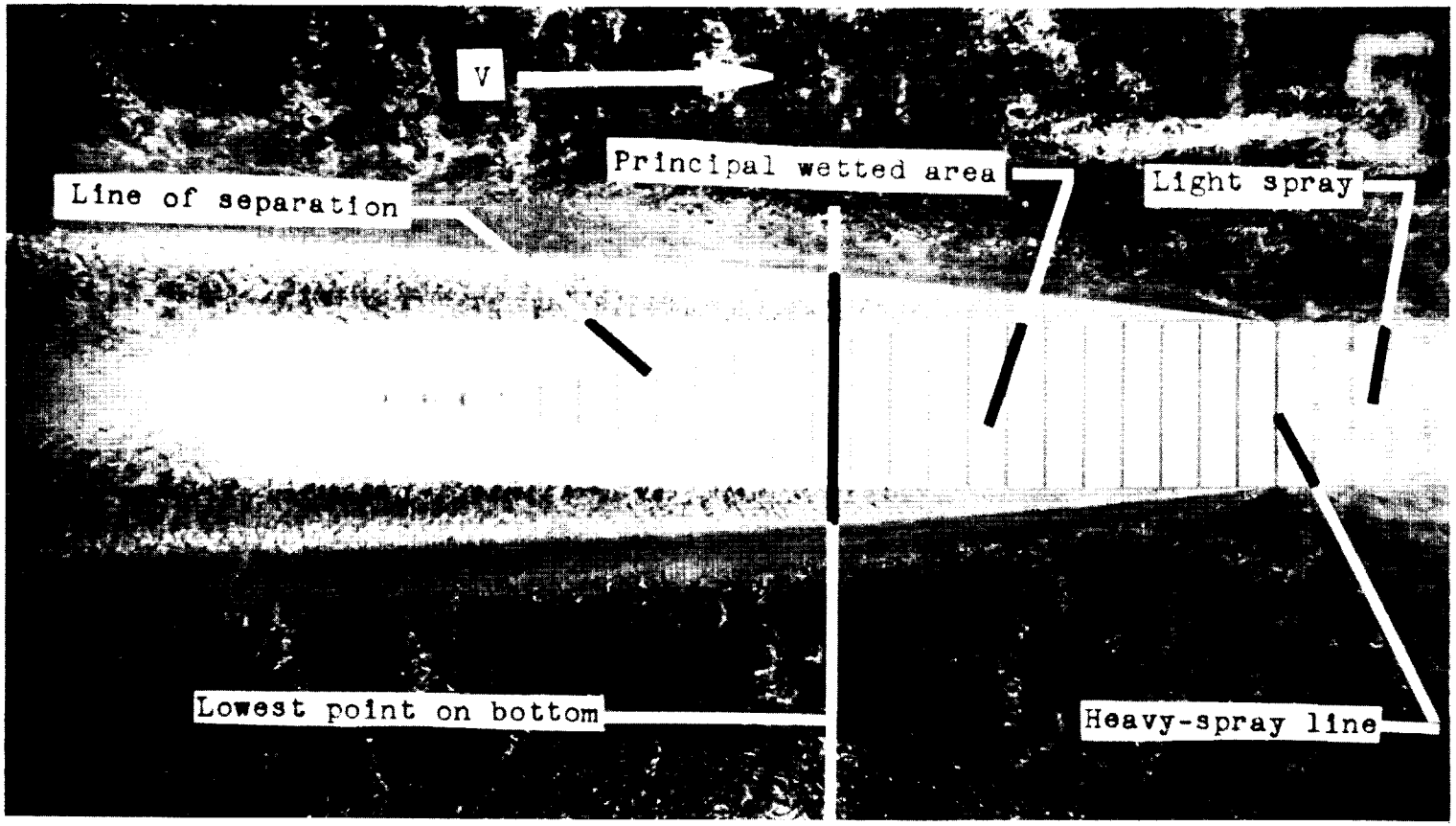

(c) At a trim τ of -11.75°. L-58-131a

Figure 3.- Concluded.

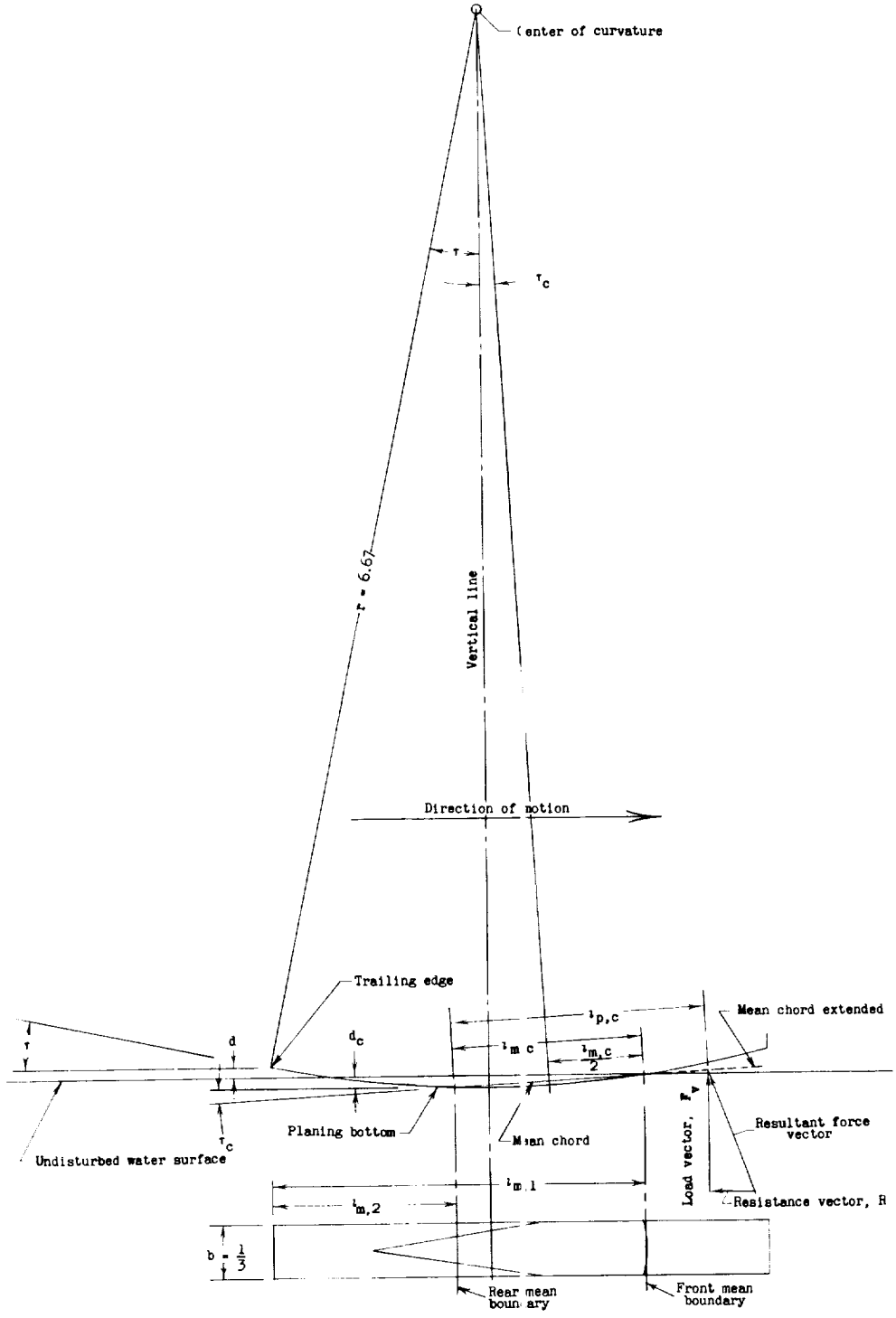

Figure 4.- Sketch of model during test run. Dimensions are in feet.

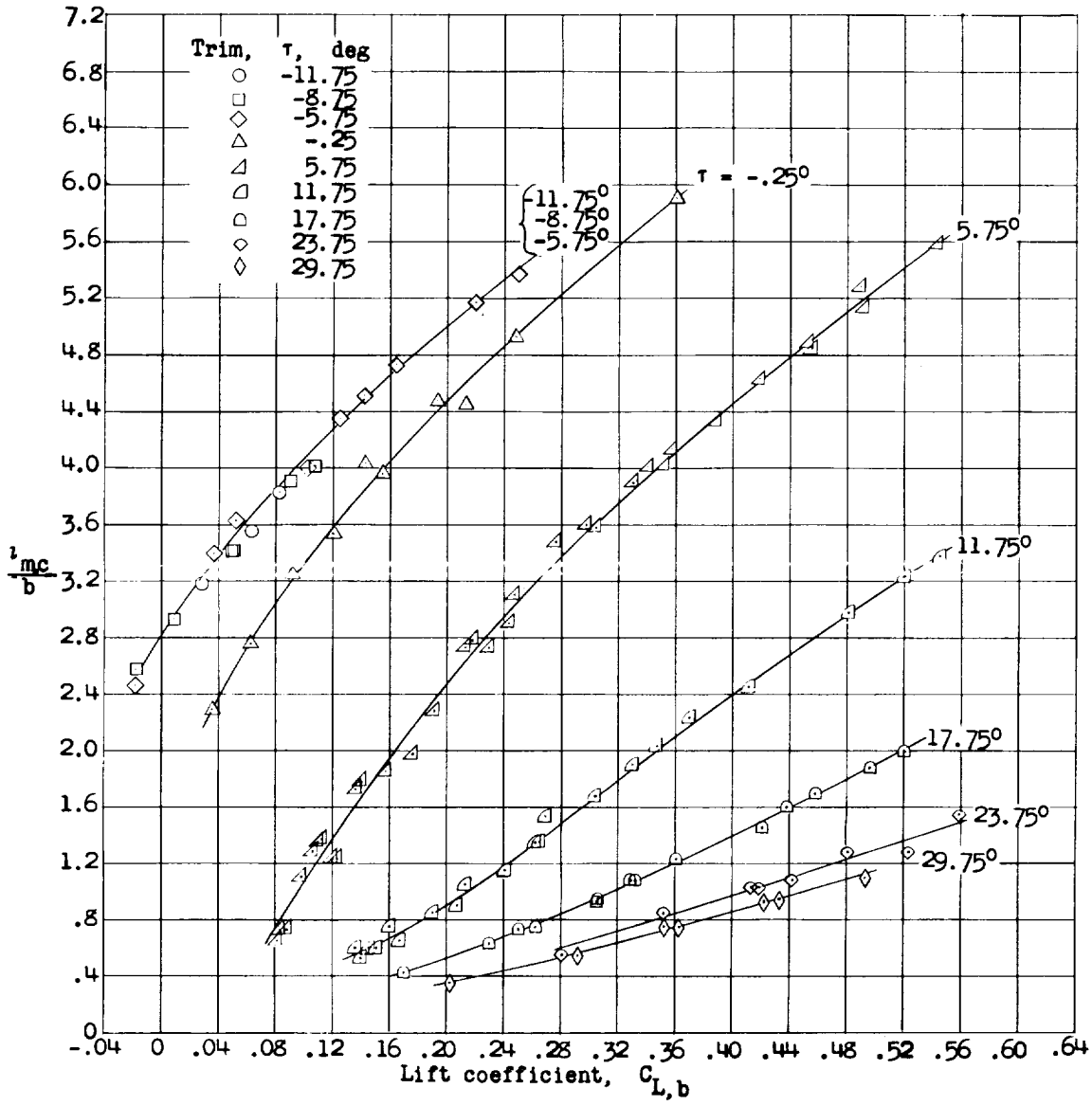

Figure 5.- Variation of mean wetted length-beam ratio with lift coefficient for several values of trim at the trailing edge.

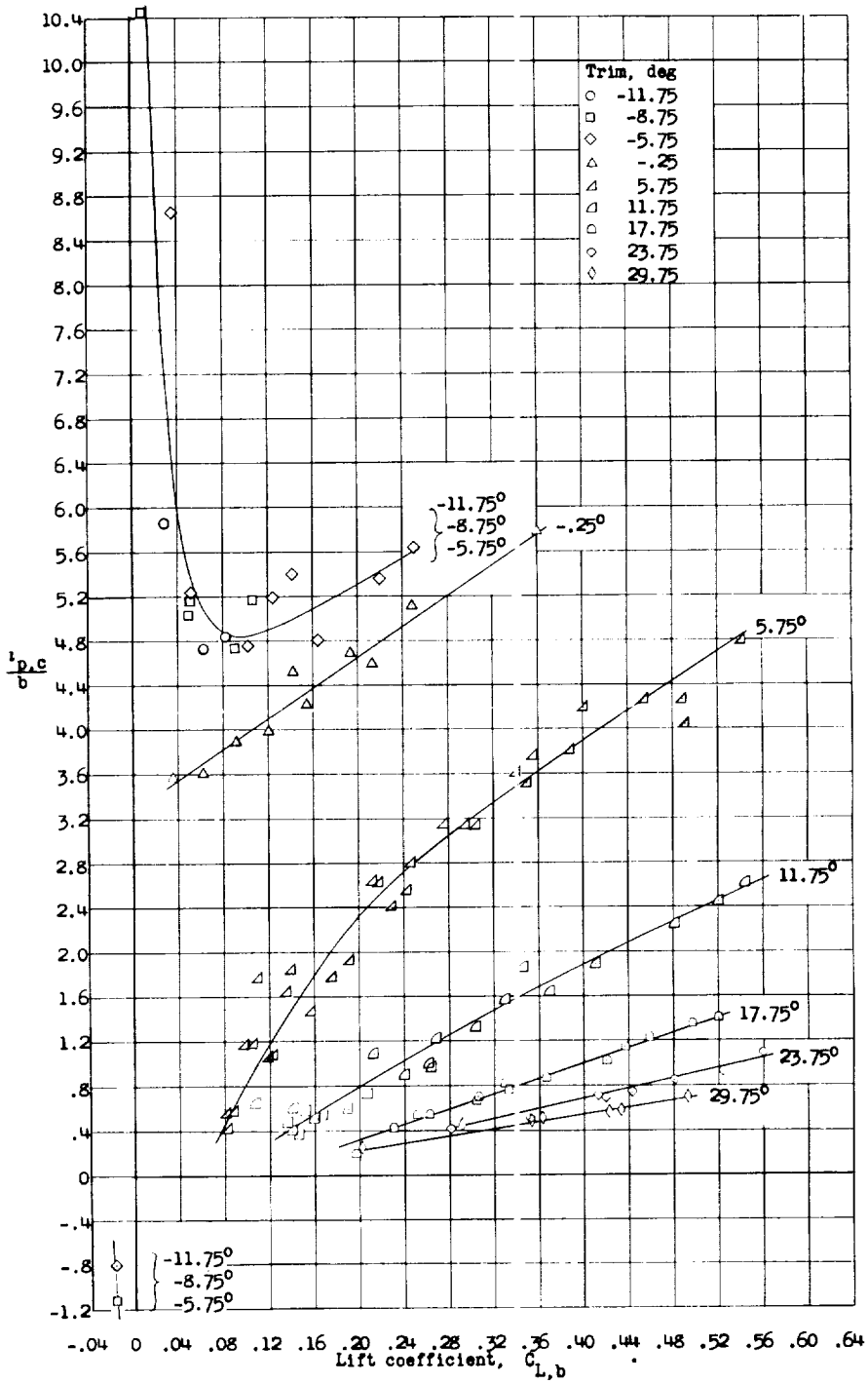

Figure 6.- Variation of nondimensional center-of-pressure location with lift coefficient.

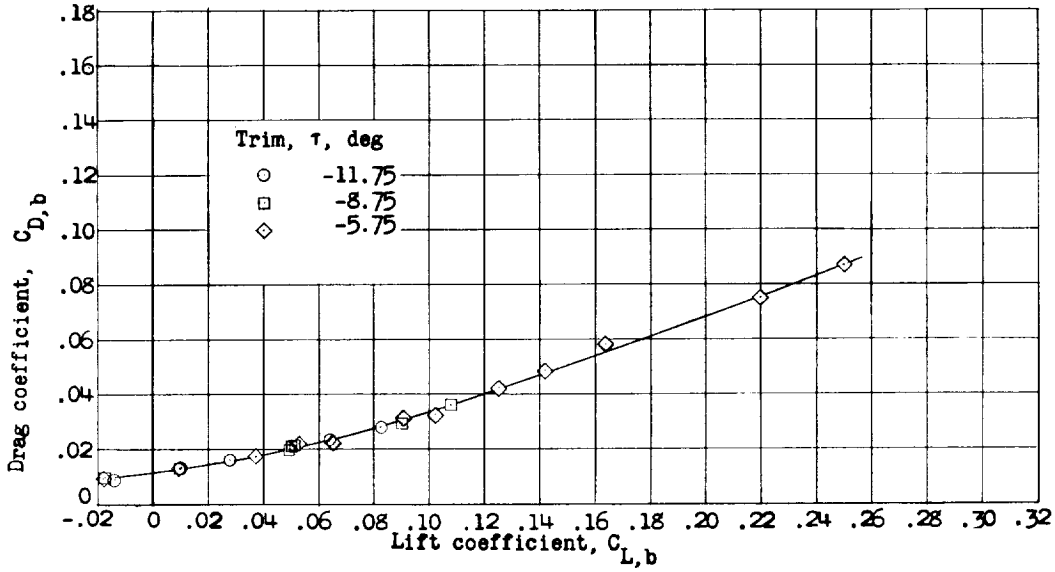

(a) Trim: -11.75°, -8.75°, -5.75°.

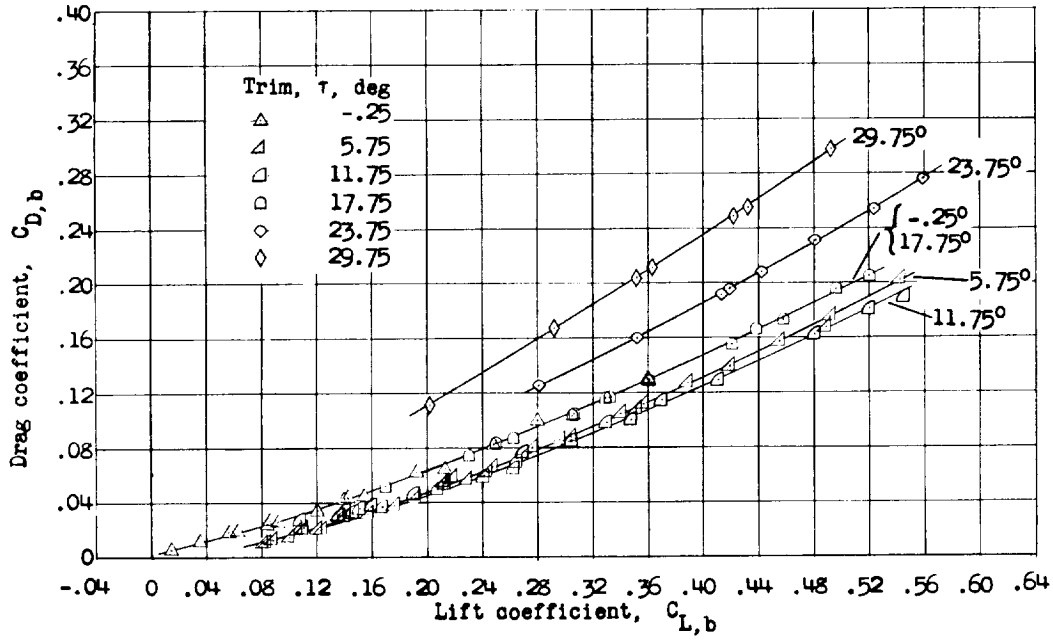

(b) Trim: -0.25°, 5.75°, 11.75°, 17.75°, 23.75°, 29.75°.

Figure 7.- Variation of drag coefficient with lift coefficient for several values of trim at the trailing edge.

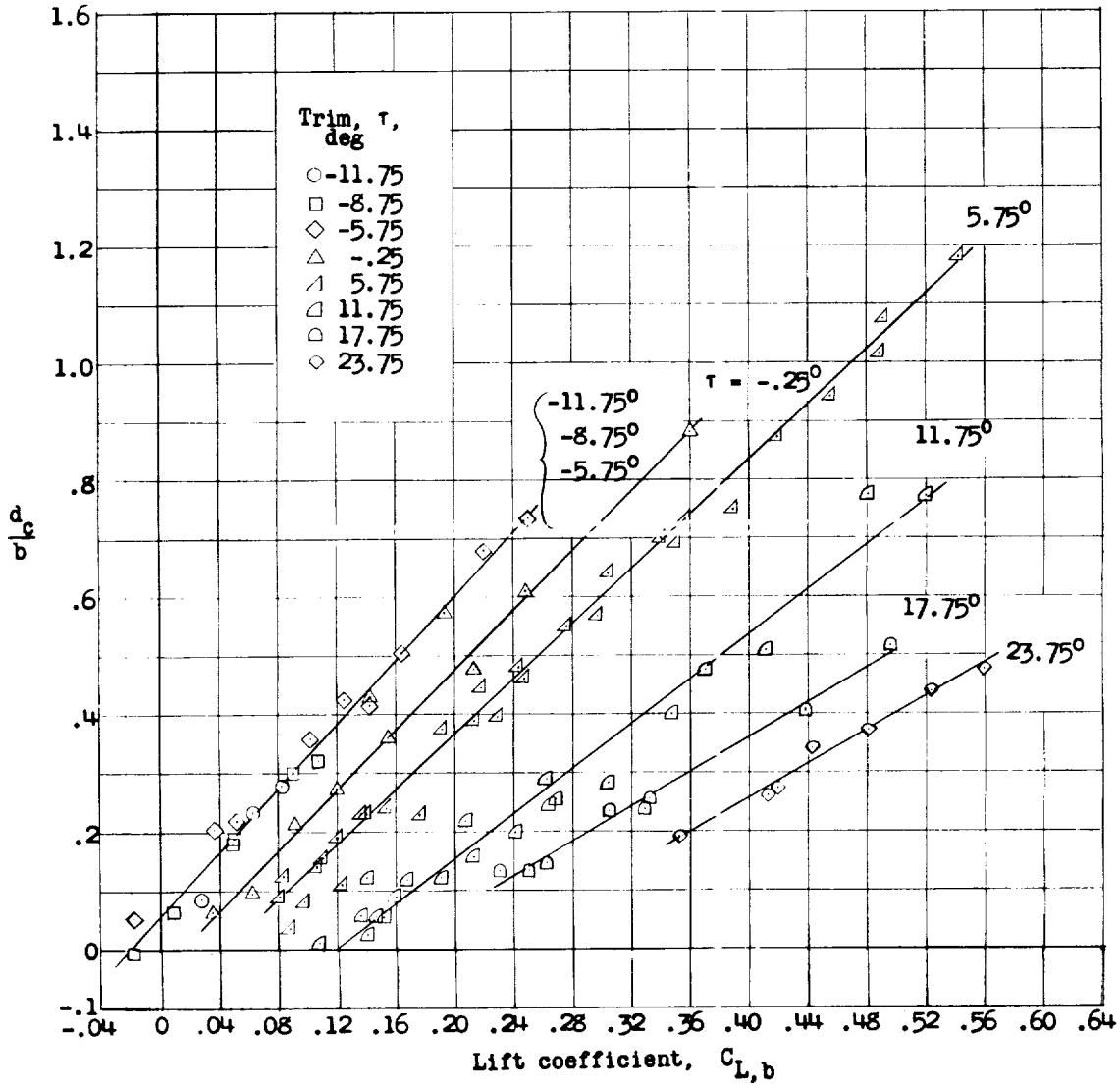

Figure 8.- Variation of nondimensional draft with lift coefficient for several values of trim at the trailing edge.

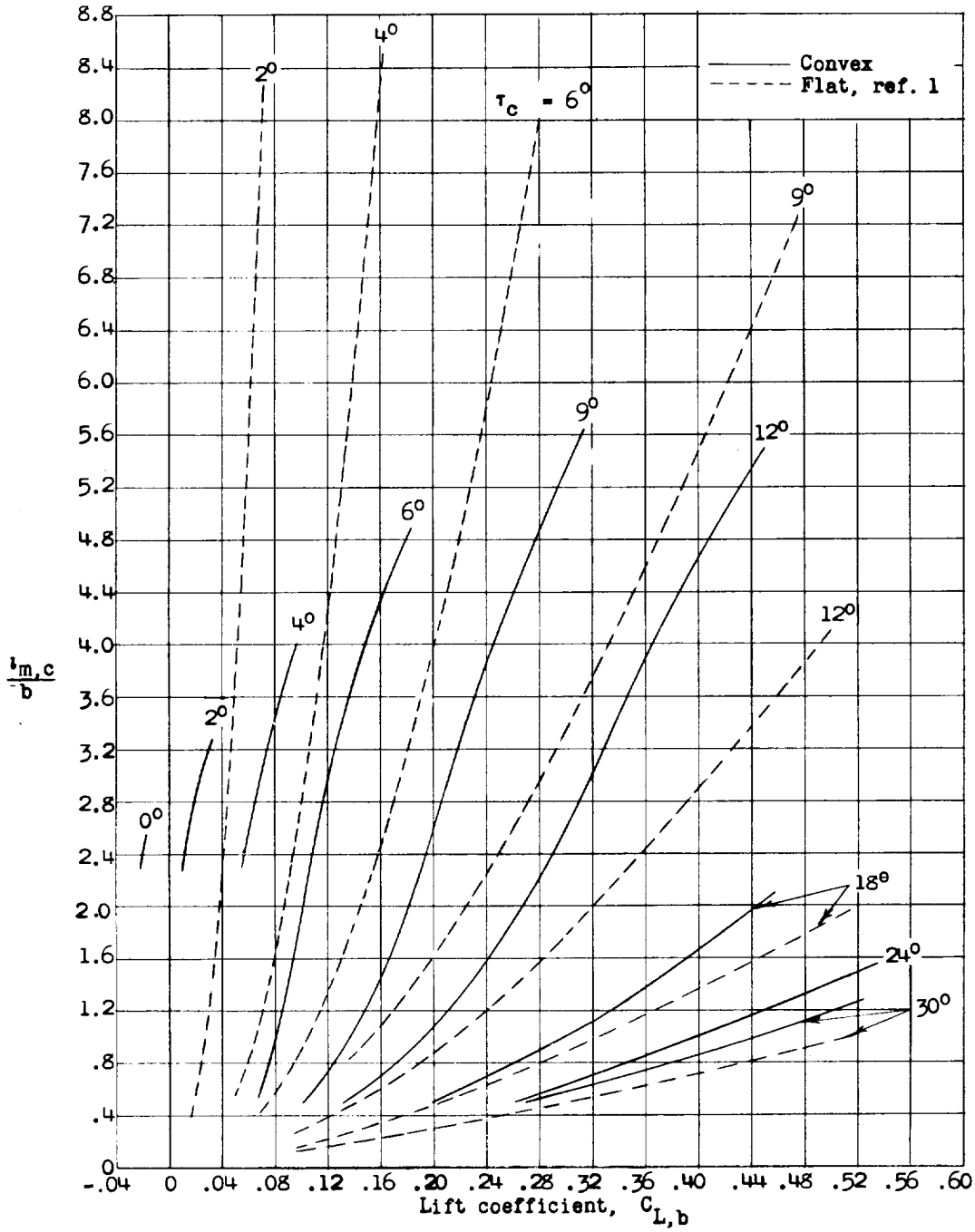

Figure 9.- Variation of the nondimensional chord of the wetted length with lift coefficient for several values of trim of the chord of the wetted length.

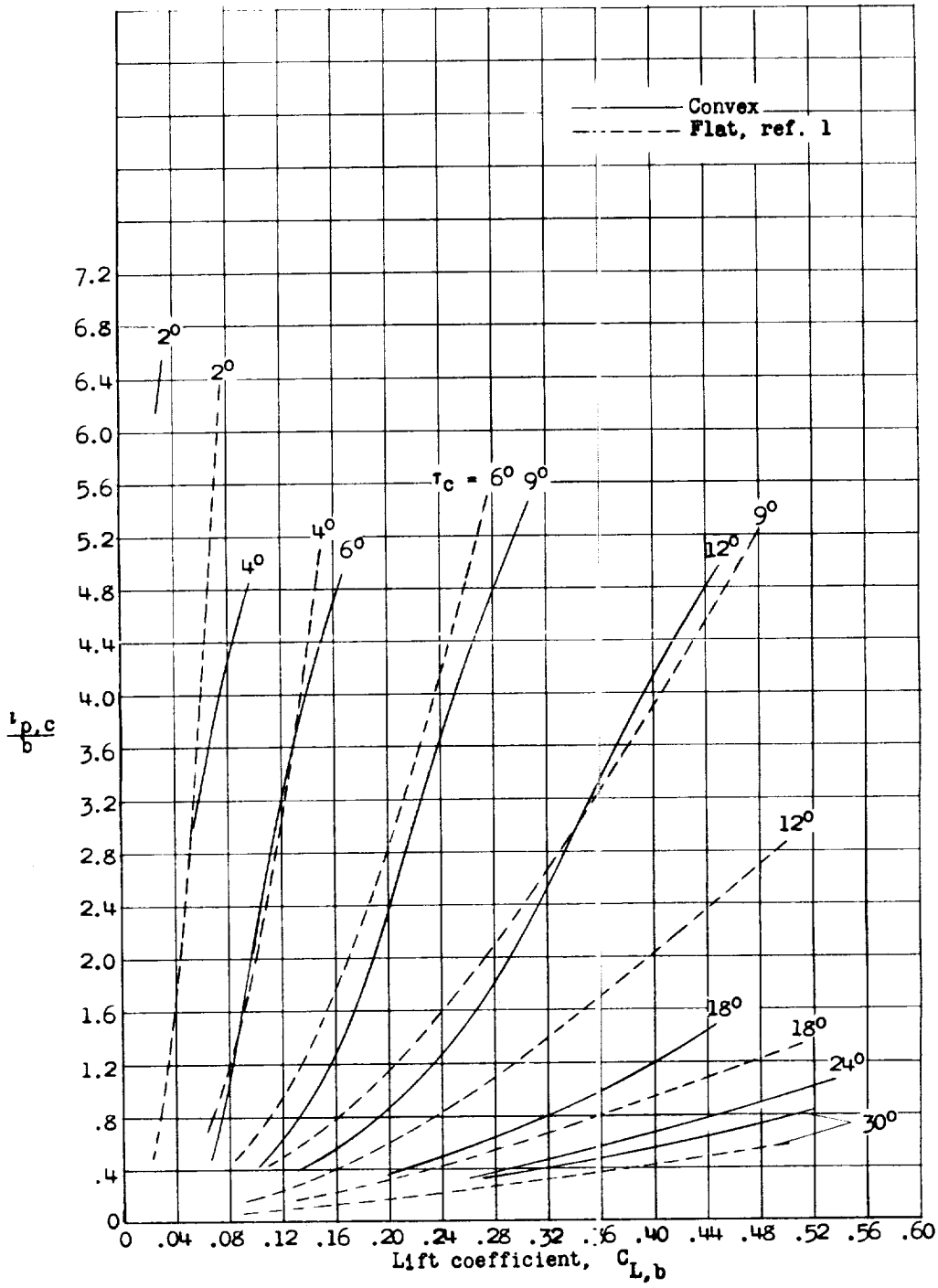

Figure 10.- Variation of nondimensional center-of-pressure location with lift coefficient for several values of trim of the chord of the wetted arc.

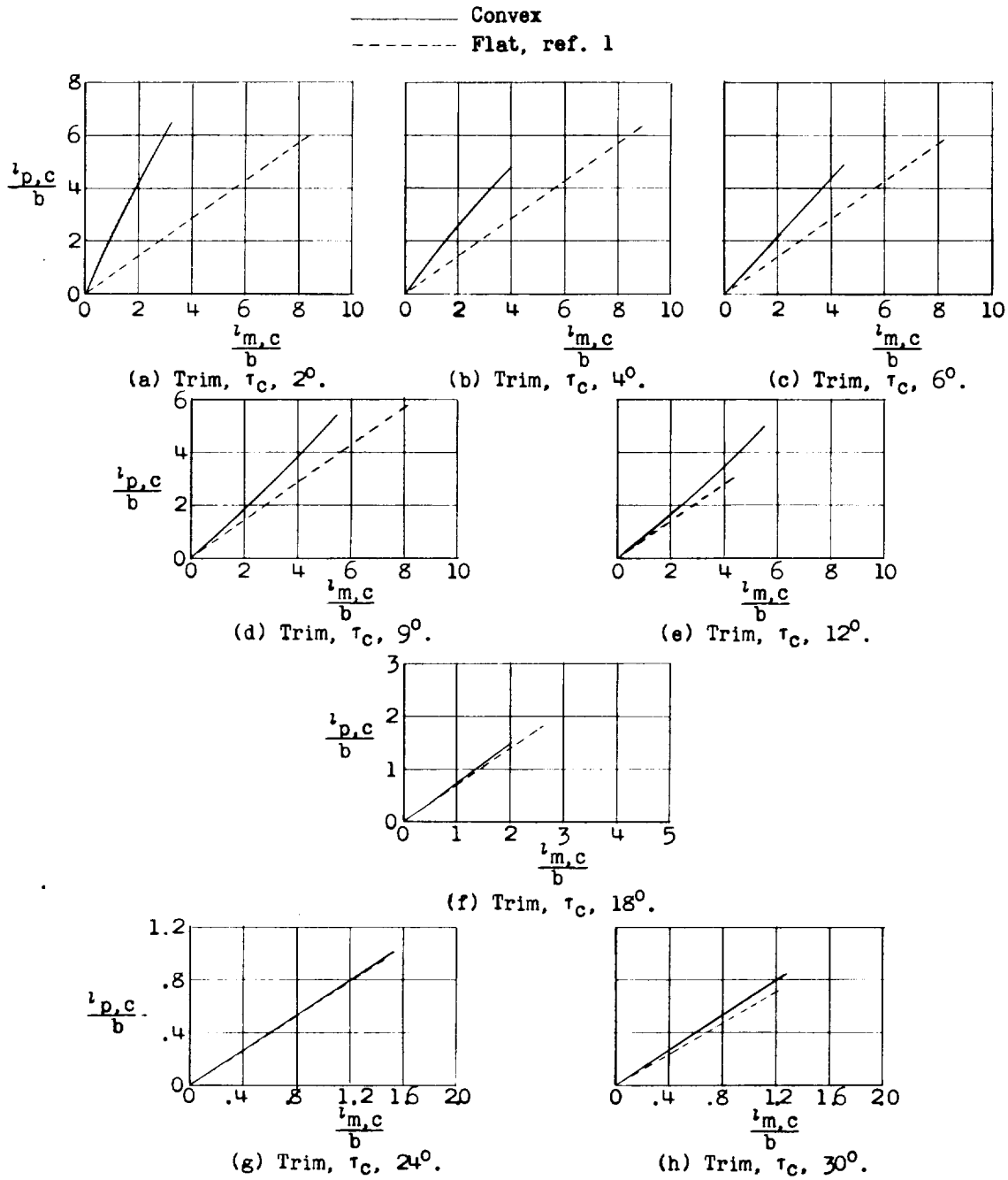

Figure 11.- Variation of nondimensional center of pressure with length-beam ratio.

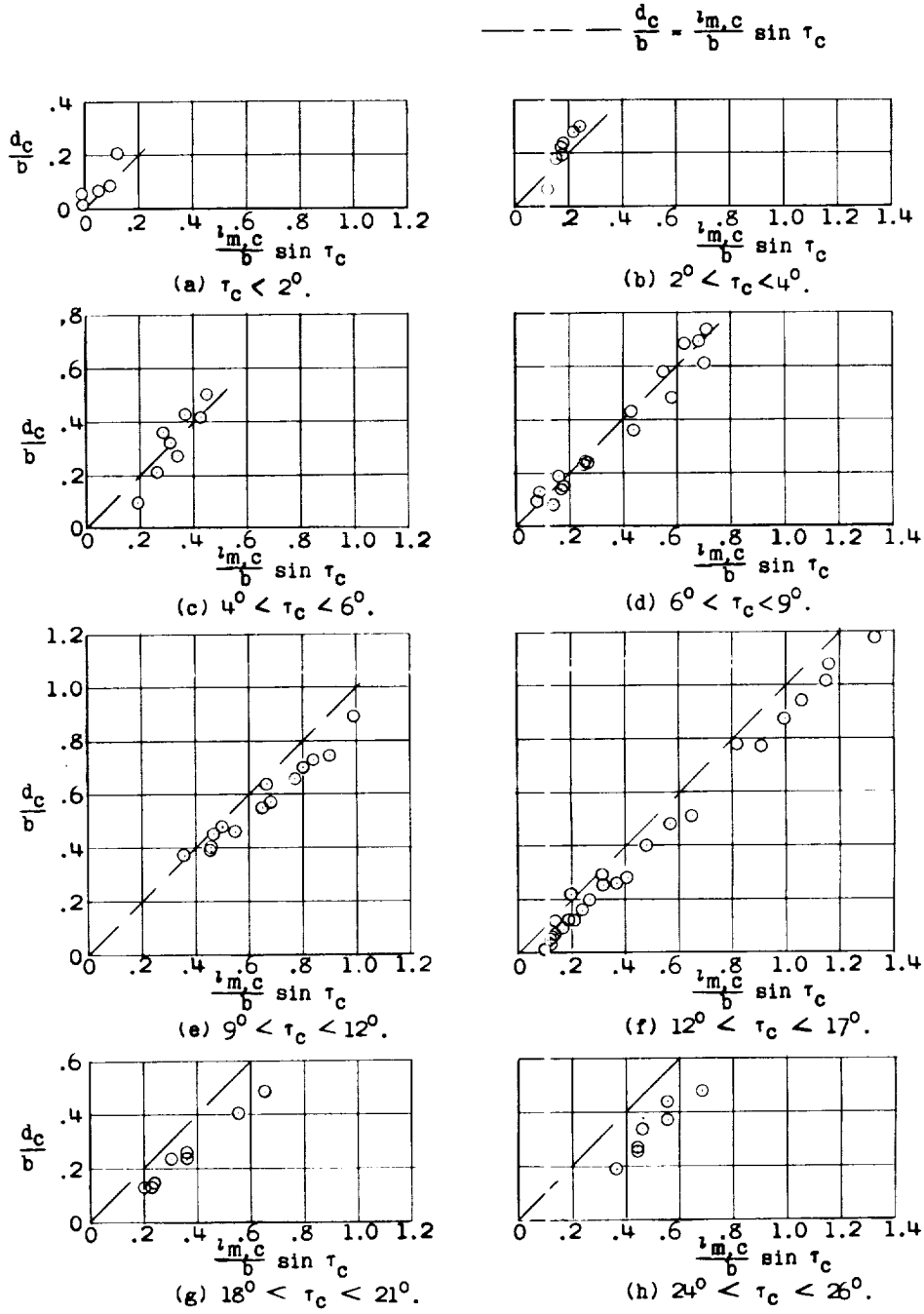

Figure 12.- Comparison of the nondimensional draft referred to the undisturbed water surface, d_c/b, with the nondimensional draft referred to the water surface at the leading edge, $\frac{l_{m,c}}{b} \sin \tau_c$ for several values of trim of the chord of the wetted arc.

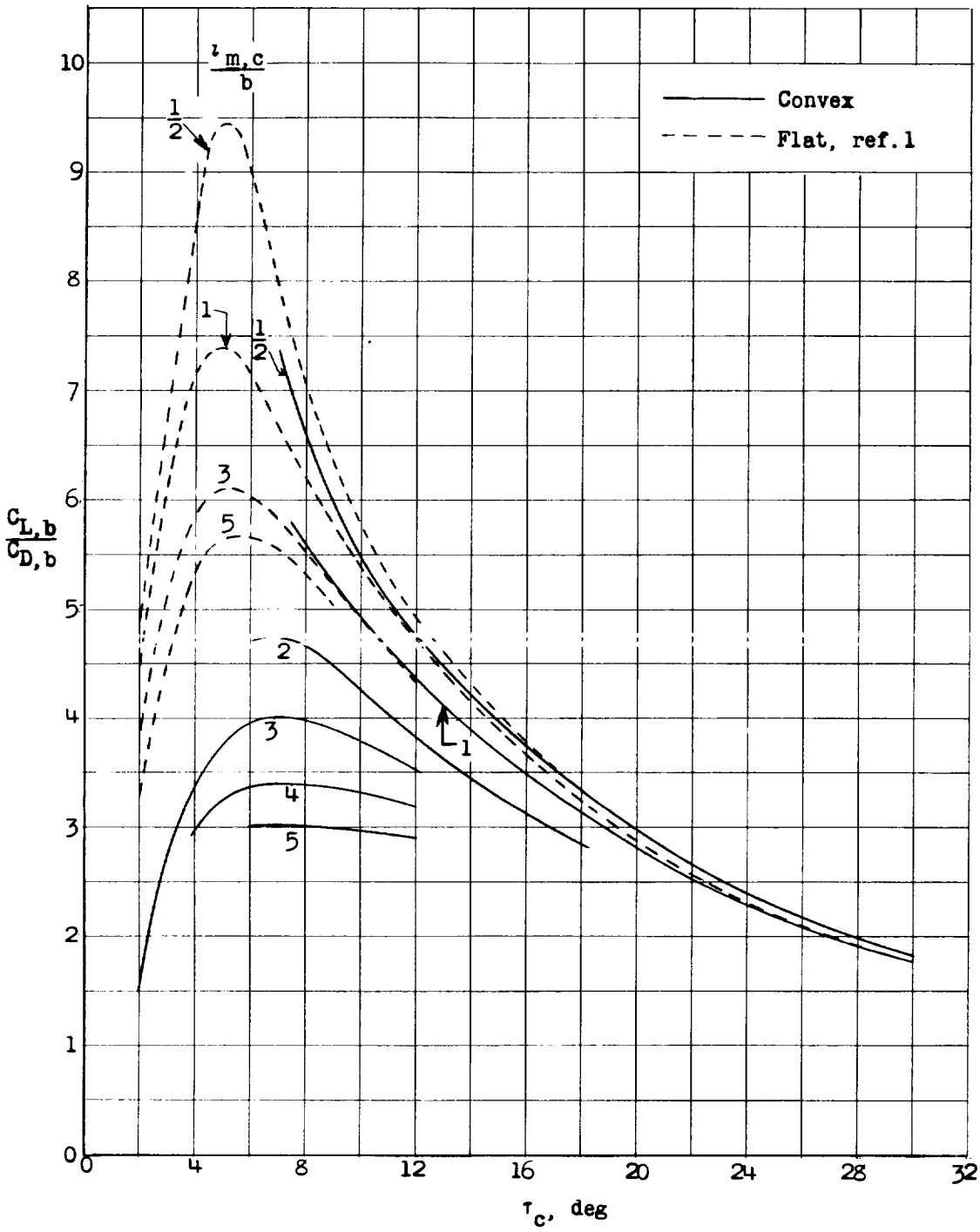

Figure 13.- Comparison of lift-drag ratios of longitudinally straight and convex surfaces.

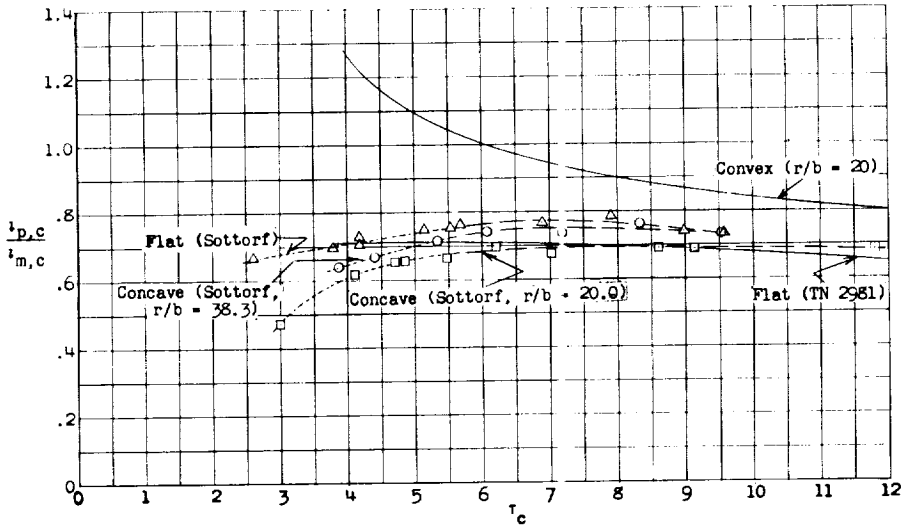

(a) Center-of-pressure location.

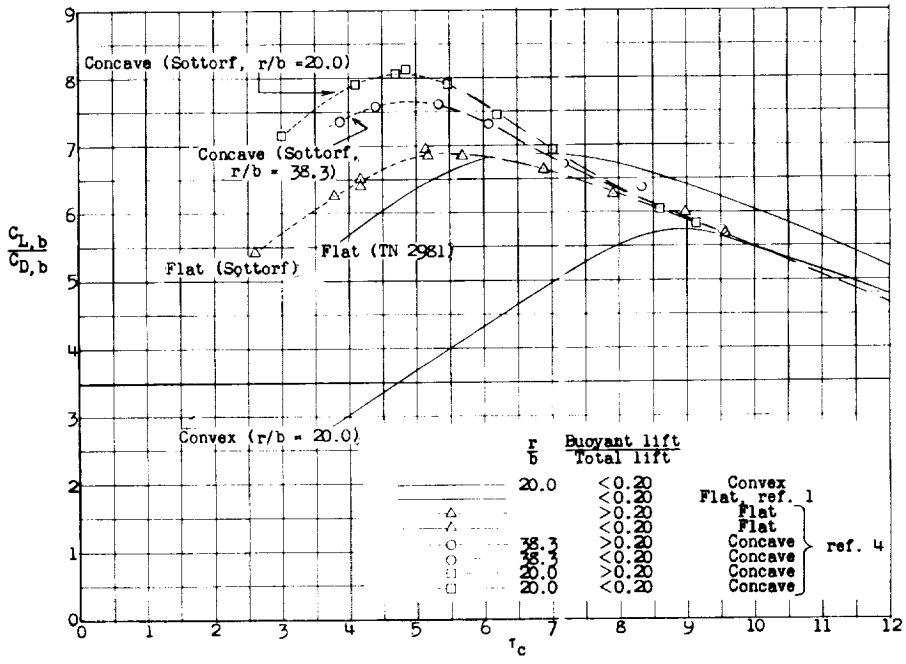

(b) Lift-drag ratio.

Figure 14.- Center-of-pressure location and lift-drag ratio of longitudinally straight, concave, and convex surfaces compared at a $C_{L,b}$ of 0.109.

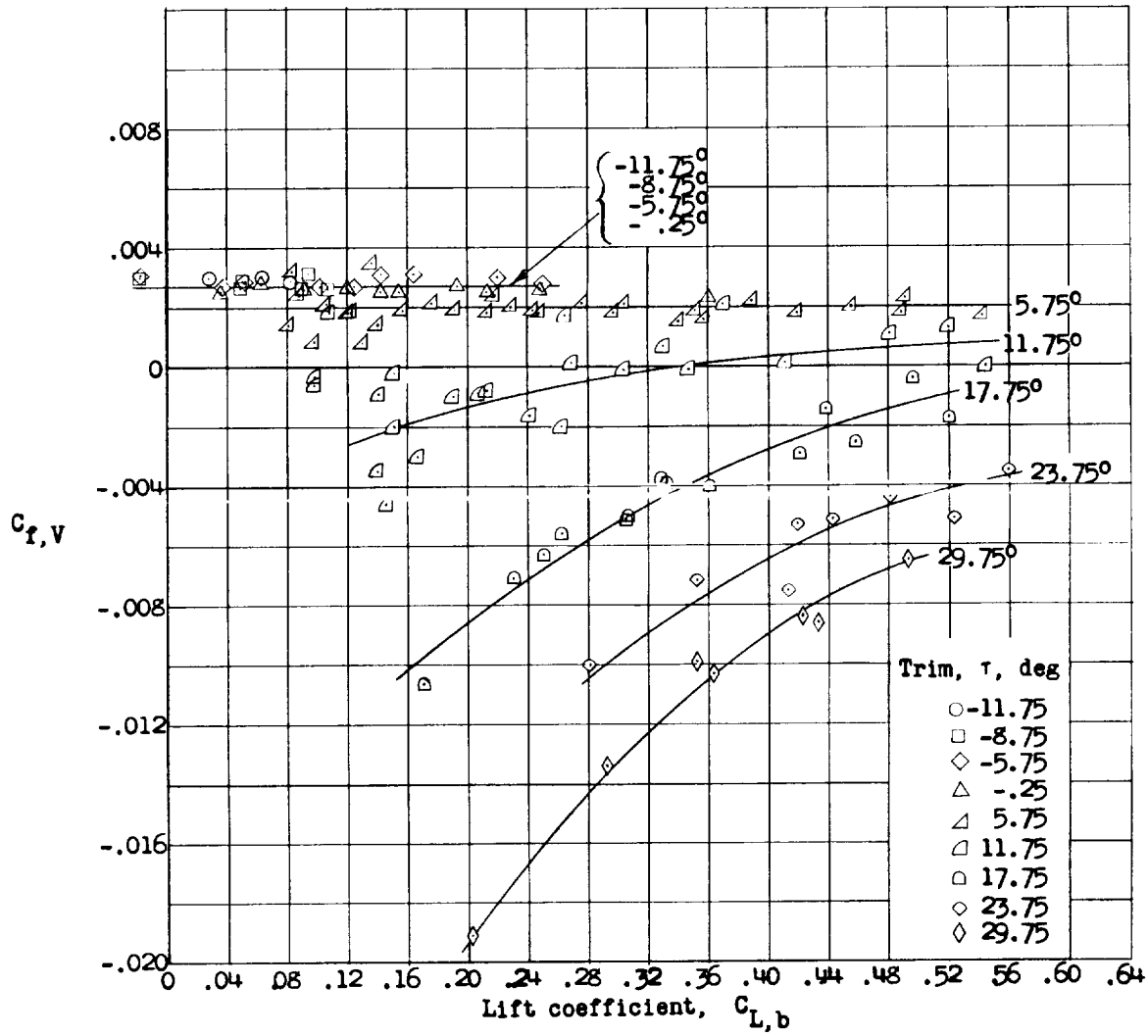

Figure 15.- Variation of nondimensional mean friction with lift coefficient for several values of trim at the trailing edge.

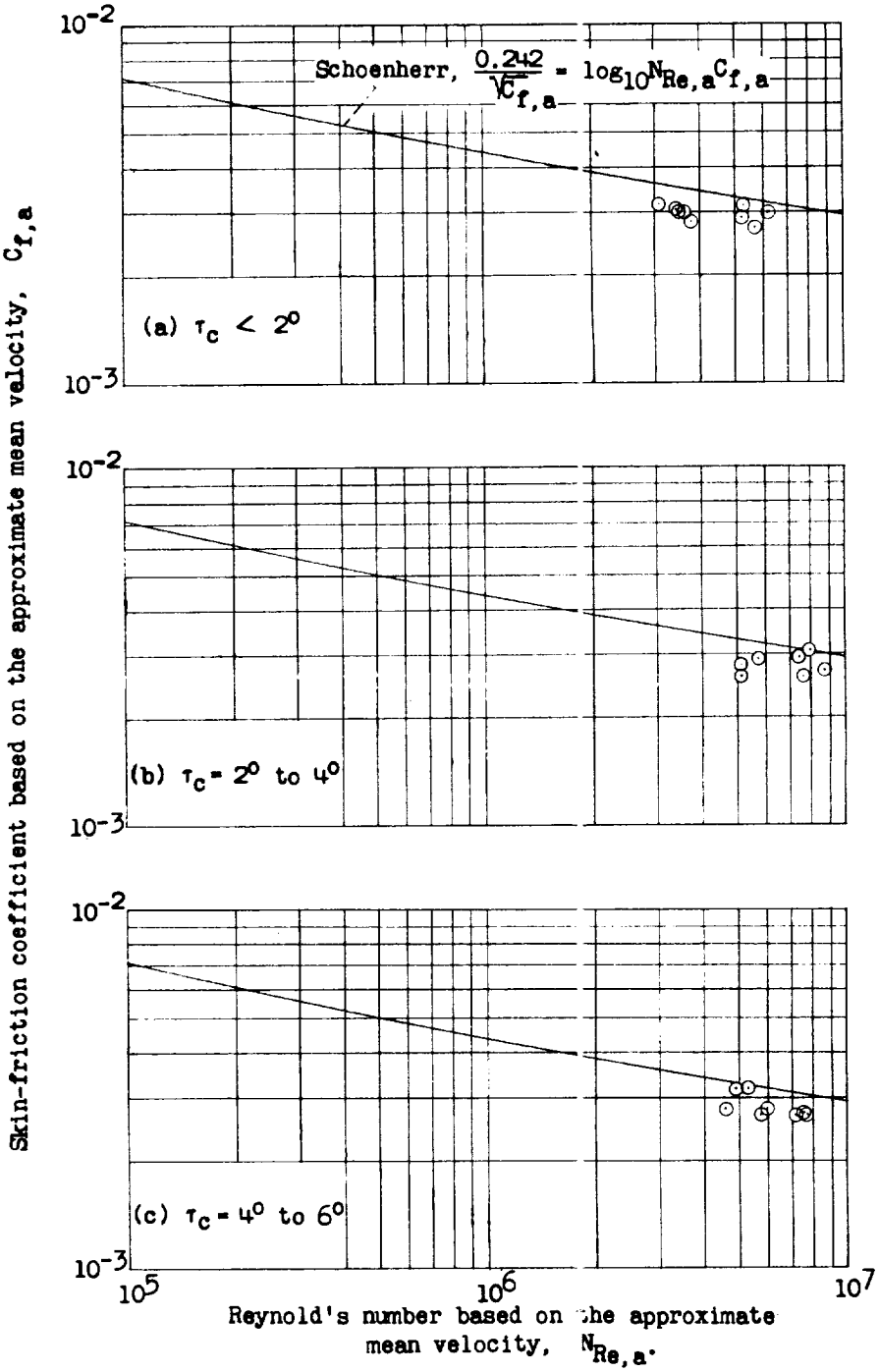

Figure 16.- Variation of skin-friction coefficient with Reynolds number.